Characterization of a human dentritic cell line; a prelude to allogeneic dendritic cell-based tumor vaccination

Santegoets, S.J.A.M.

2008

document version
Publisher's PDF, also known as Version of record

CHAPTER 7

Inducing anti-tumor T cell immunity: comparative functional analysis of interstitial versus Langerhans dendritic cells in a human cell line model

Saskia J.A.M. Santegoets
Hetty J. Bontkes
Anita G.M. Stam
Farien Bhoelan
Janneke J. Ruizendaal
Alfons J.M. van den Eertwegh
Erik Hooijberg
Rik J. Scheper
Tanja D. de Gruijl

Submitted for publication

Abstract

Dendritic cells (DC) are increasingly applied as a cellular adjuvant in immunotherapy of cancer. Two major myeloid DC subsets are recognized: Interstitial DC (IDC) that infiltrate connective tissues and Langerhans cells (LC) that line epithelial surfaces. Yet, functional differences between IDC and LC remain to be defined. We recently showed that the CD34+ acute myeloid leukemia cell line MUTZ-3 supports differentiation of both DC-SIGN+ IDC and Langerin+, Birbeck granule-expressing LC. By comparative functional characterization of MUTZ-3 IDC and LC, we aimed to elucidate the relative abilities of these two DC subsets to induce a specific T cell response and reveal the more suitable candidate for use as a clinical vehicle of tumor vaccines. While mature LC and IDC displayed comparable lymph node-homing potential, mature LC showed higher allogeneic T cell stimulatory capacity. Nevertheless, IDC supported the induction of tumor antigen-specific CD8+ T cells at an overall higher efficiency. This might be related to the observed inability of LC to release T cell stimulatory cytokines such as IL-12p70, IL-23 and IL-15. Although this inability did not result in a detectable deviation in the cytokine expression profile of primed T cells, transduction with IL-12p70 significantly improved priming efficiency of LC, and ensured a functional equivalence with IDC in this regard. In conclusion, except for the inability of LC to release distinct type-1 T cell-stimulatory cytokines, *in vitro* functions of LC and IDC suggest comparable abilities of both subsets for the *in vivo* induction of anti-tumor T cells.

Introduction

Dendritic cells (DC) are professional antigen presenting cells (APC) with the unique ability to initiate primary T cell responses (1-3). Myeloid DC differentiate from CD34+ hematopoietic progenitor cells (HPC) and can develop into two recognized subsets, Langerhans cells (LC), which are mostly found in the epidermis, and Interstitial DC (IDC), which are mostly located in connective tissues (4,5). Because of their critical role in orchestrating the immune response, DC have been used as a cellular adjuvant in immunotherapy of cancer. Numerous animal studies have shown that administration of tumor-antigen loaded DC could induce protective immunity in naive animals (6-8), as well as tumor regression and tumor-free survival in mice bearing established tumors (9). The immunogenicity of DC has also been shown in human clinical trials. Initially, DC vaccination studies were performed with DC directly isolated from peripheral blood (10,11). Major disadvantages of this approach were the low yields of DC (11), the variety of peripheral blood DC subsets (12) and the varying percentages of these DC subsets in cancer patients. The development of methods to generate DC from CD34+ HPC progenitors (CD34-DC) or CD14+ monocytes (MoDC) *in vitro*, have facilitated DC vaccination studies tremendously. Numerous clinical trials, employing either MoDC or CD34-DC, have demonstrated the feasibility and safety of DC-based vaccination approaches, of which some reported encouraging clinical responses (13-16).

So far, in the vast majority of clinical trials MoDC have been used for vaccination, while only few trials have made use of CD34-DC (as reviewed by Davis *et al*. (17)). However, it has been suggested that CD34-DC are more effective as compared to MoDC in clinical DC vaccination studies (15), as well as in *in vitro* antigen-specific T cell stimulation (18). The beneficial effect of these CD34-DC might be

due to the presence of “contaminating” LC in the CD34-DC preparations. This hypothesis was supported by Ratzinger and co-workers, demonstrating that CD34-LC exhibit a superior capacity to induce influenzavirus- and tumor-specific CTL *in vitro*, compared to MoDC and CD34-DC (both belonging to the IDC subset) (19). For clinical DC vaccination purposes however, functional differences between IDC and LC remain to be characterized more extensively, not only at the level of T cell priming, but also for their capacity to migrate towards lymph nodes and their ability to release T cell-stimulatory cytokines and skew Th1/Th2 cytokine profiles. Such extensive comparative studies are hampered by difficulties in the generation of large amounts of Birbeck granule-containing, Langerin+ LC. We have previously shown that DC-SIGN+ IDC and *bona fide* Langerin+/Birbeck granule+ LC can be generated from the MUTZ-3 cell line, a human CD34+ acute myeloid leukemia cell line (20,21). In addition, we observed equivalent *in vitro* T cell priming efficiencies for autologous MoDC and MUTZ-3 IDC, matched for HLA-A2 or -A3 expression, both generating functional tumor-specific CTL (22). These observations indicate the validity of the MUTZ-3 cell line model, which facilitates extensive head-to-head comparative functional studies of IDC versus LC.

In the current study we characterized functional properties crucial for the *in vivo* generation of CTL-mediated immunity of MUTZ3-derived IDC and LC. Our data show that both DC subsets are capable of tumor-specific CTL induction. However, T cell priming efficiency of IDC was superior compared to LC, most likely due to the inability of LC to release type-1 T cell-stimulatory cytokines. Indeed, transduction with IL-12p70 significantly enhanced the CTL priming efficiency of LC and ensured a functional equivalence with IDC in this regard. We conclude that both DC subsets are valid vaccine vehicles for tumor immunotherapy, but that provision of type-1 T cell stimulatory cytokines such as IL-12p70 is required to ensure optimal T cell stimulation, particularly by LC.

Materials and Methods

Cell Lines

The human CD34+ acute myeloid leukemia cell line MUTZ-3 (Deutsche Sammlung von Mikroorganismen und Zellkulturen [DSMZ], Braunschweig, Germany) was cultured as described previously (20,22). The EBV-transformed B cell line JY and the TAP-deficient cell line T2 (both HLA-A2+) were cultured in IMDM (BioWhittaker, Verviers, Belgium) supplemented with 10 % fetal bovine serum (Perbio, Helsingborg, Sweden), 100 I.E./ml sodium penicillin (Yamanouchi Pharma, Leiderdorp, The Netherlands), 100 μg/ml streptomycin sulphate (Radiumfarma-Fisiopharma, Naples, Italy), 2.0 mM L-glutamine (Invitrogen, Breda, The Netherlands) and 0.01 mM 2-mercapoethanol (Merck, Darmstadt, Germany) (i.e. complete medium). The prostate cancer cell line PC-3, the colon carcinoma cell line SW620, the glioblastoma cell line U251 and the melanoma cell lines Mel-JKO and Mel-AKR were cultured in DMEM complete medium.

Synthetic Peptides

The HLA-A2-restricted peptides $CEA_{571-579}$ (YLSGANLNL), $PSA_{146-154}$ (KLQCVDLHV), Her-$2/neu_{369-377}$ (KIFGSLAFL), MART-1_{26-35L} (ALGIGILTV) and Bcr-$abl_{926-934}$ (SSKALQRPV) were

synthesized by solid-phase strategies on an automated multiple peptide synthesizer (Syro II, MultiSyntech, Witten, Germany) using Fmoc-chemistry. Peptides were analyzed by reversed-phase high performance liquid chromatography (HPLC), dissolved in DMSO (Merck) and stored at –20ºC.

Retroviral IL-12p70 transduction of MUTZ-3

The IL-12elasti cassette containing the p35 and p40 subunits of IL-12 joined together by a flexible linker (InvivoGen, San Diego, CA) was introduced into MUTZ-3 cells by retroviral transduction. The truncated, signaling defective form of the Nerve growth factor receptor (ΔNGFR) was used as a marker gene for transduced cells. The retroviral vector LZRS-IL-12-IRES-ΔNGFR, constructed by replacing the hTERT ORF from the LZRS-hTERT-IRES-ΔNGFR construct (23) with the IL-12elasti cassette, was used to produce the retroviral supernatant. Retroviral transduction of MUTZ-3 was performed as described previously (24). Briefly, 5 x 10^5 MUTZ-3 cells, were resuspended in retroviral supernatant supplemented with 10% 5367 conditioned medium and transferred to a fibronectin (RetroNectin; Takara, Otsu, Japan)-coated well of a non-tissue-culture-treated 24-well plate (BD Biosciences). Plates were centrifuged, followed by 5-h incubation at 37°C. The next day, retroviral transduction was repeated. A NGFR-specific antibody (Chromoprobe, Aptos, CA) was used to analyze transduction efficiency and isolate transduced cells by flow sorting.

In vitro Generation of Monocyte-Derived and MUTZ-3-Derived Interstitial and Langerhans-like Dendritic Cells

MoDC, MUTZ-3 IDC, MUTZ-3-LC and MUTZ-3-IL-12-derived IDC and LC (hereafter referred to as MUTZ-3-IL-12 IDC and LC), were generated as described (20,21,25). At day 7 or day 10, maturation of MoDC, MUTZ-3 IDC and LC was induced by adding a cytokine cocktail consisting of 50 ng/ml TNF-α, 100 ng/ml IL-6, 25 ng/ml IL-1β (hereafter referred to as MCM mimic; Strathmann Biotec, Hamburg, Germany), with or without 1 μg/ml PGE2 (Sigma-Aldrich, St. Louise, MO) or by adding a type-1-polarizing cytokine cocktail containing 50 ng/ml TNF-α, 25 ng/ml IL-1β, 1000 U/ml IFN-γ, 20 μg/ml poly-I:C (Sigma) and 3000 U/ml IFN-α (Peprotech, London, UK) (hereafter referred to as IFN-α/p-I:C type-1 cytokine cocktail (26)).

Antibodies, Tetramers and Flow Cytometry

PE- or FITC-labeled Abs directed against human CD34 (Strathmann Biotec), CD40, CD83, CD8β, Langerin, TCRαβ, TCRγδ (Immunotech, Marseille, France), CD1a, CD8α, CD14, CD28, CD27, CD45RA, CD54RO, CD54, CD62L, CD80, CD86, CCR7 (2H4), DC-SIGN, HLA-DR (all from BD Biosciences, Mountain view, CA) were used for flow cytometric analysis. PE- and/or APC-labeled HLA-A2 tetramers (Tm) presenting the CEA_{571}, PSA_{146}, $MART\text{-}1_{26L}$ and $Her\text{-}2/neu_{369}$ epitopes were prepared as described previously (27). Antibody and/or tetramer staining was performed in PBS supplemented with 0.1% BSA and 0.02% natrium-azide for 30 minutes at 4ºC and 15 minutes at 37 ºC respectively. Stained cells were analyzed on a FACScalibur (BD Biosciences) using Cell Quest software. To exclude dead cells in flow cytometric tetramer analysis, 0.5 μg/ml propidium iodide (ICN Biomedicals, Zoetermeer, The Netherlands) was used.

Primary CTL Induction in vitro

Antigen-specific CD8+ T cells were generated as described, with some minor modifications (22,23). In brief, mature MUTZ-3 IDC and MUTZ-3 LC, either derived from wild-type MUTZ-3 or IL-12-transfected MUTZ-3, were loaded with 1 μg/ml peptide in the presence of 3 μg/ml β2-microglobulin (Sigma-Aldrich, St. Louise, MO) for 2-4 hours at room temperature and irradiated (40 Gy). $1x10^5$ peptide-loaded DC were cultured for 10 days with $1x10^6$ CD8β+ CD8+ T precursors and $1x10^6$ irradiated (80 Gy) CD8β$^-$ autologous PBMC in Yssel's medium (28) supplemented with 1% hAB serum (ICN Biochemicals), 10 ng/ml IL-6 and 10 ng/ml IL-12 (in experiments with wild-type MUTZ-3 IDC/LC) in a 24 well tissue-culture plate. At day 1, 10 ng/ml IL-10 (R&D Systems, Minneapolis, MN) was added. After 10 days, CD8+ T cell cultures were re-stimulated with $1x10^5$ fresh MUTZ-3 IDC or LC, loaded with 10 ng/ml peptide, in the presence of 5 ng/ml IL-7 (Strathmann Biotec). From day 17 onwards, CD8+ T cell cultures were stimulated weekly with $1x10^5$ peptide-loaded JY cells, unless indicated otherwise. Two days after each restimulation, 10 U/ml IL-2 (Strathmann Biotec) was added. One day prior to each restimulation, a sample was taken and analyzed by flow cytometry using both PE- and APC-labeled tetramers presenting the relevant epitope. Tetramer-positive CD8+ T cells were isolated by tetramer+ magnetic cell sorting and subsequently expanded. For this purpose, CD8+ T cells were weekly stimulated with irradiated feeder-mix consisting of allogeneic PBMC and JY cells in Yssel's medium supplemented with 100 ng/ml phytohaemagglutin (PHA; Murex Biotech, Dartford, U.K.) and 20 U/ml IL-2.

Intracellular IFN-γ detection

To determine the capacity of the CD8+ T cells to produce IFN-γ upon recognition of a specific target, intracellular IFN-γ staining was performed. CD8+ T cells were cultured with target cells at an effector:target cell (E:T) ratio of 2:1 in 96-well round-bottom plate in the presence of 0.5 μl of GolgiPlug (BD Biosciences). After 5 hours, cells were harvested, washed, stained with APC-labeled tetramer and PE-labeled anti-CD8 mAb. After fixation with cytofix/cytoperm solution and permeabilization with Perm/wash solution (both from BD Biosciences), cells were labeled with FITC-conjugated anti-IFN-γ Ab (BD Biosciences). Stained cells were analyzed on a FACScalibur.

Chromium Release Assay

Cytotoxic activity of CD8+ T cell lines was determined by standard chromium release assay as described (23).

Mixed Leukocyte Reaction (MLR)

T cell stimulatory capacity of MUTZ-3 IDC and LC was determined by allogeneic MLR as described (21).

Transwell migration assay

Chemotaxis of mature MoDC, MUTZ-3 IDC and MUTZ-3 LC was measured by migration through a polycarbonate filter of 5 μm pore size. For this purpose, 100,000 mature MoDC, MUTZ-3 IDC or

MUTZ-3 LC were seeded in serum-free medium in the upper well of a 24-well transwell chamber and allowed to migrate for 4 hours towards serum-free medium alone or serum-free medium containing 250 ng/ml of the chemokines CCL19 (Peprotech) or CCL21 (Biosource International, Camarillo, CA). After 4 hours, the migrated cells were harvested and counted by flow cytometry by adding a fixed number of fluorescent flow count beads (Beckman Coulter, Galway, Ireland). The absolute number of migrated cells was expressed as: [total number of cells counted ∗ total number of added beads] / total number of counted beads.

Cytokine release by Dendritic Cells

Immature MoDC, MUTZ-3 IDC and LC were analyzed for the release of IL-12p70, IL-10 and IL-15 as described previously (26,29). Briefly, for IL-12 and IL-10 production, the different DC subsets were stimulated for 8 hours in a 96-well round-bottom culture plate in IMDM + 10% FCS with either MCM mimic with or without PGE2 or the IFN/α-p-I:C type-1-polarizing cytokine cocktail, followed by a 16 hours stimulation with the CD40L-transfected J558 cell line in the presence or absence of 1000 U/ml IFN-γ (R&D systems). IL-12p70 production by MUTZ-3-IL-12 IDC and LC was determined in the absence of CD40 ligation. To do so, MUTZ-3-IL-12 IDC and LC were stimulated for 48 hours with MCM with TNF-α. After cytokine removal, cells were cultured for an additional 24 hours and supernatants were collected. For IL-15 production, the different DC subsets were stimulated for 20 hours with either MCM mimic with or without PGE2 or the IFN-α/p-I:C type-1-polarizing cytokine cocktail. Next day, the supernatants were harvested and analyzed by enzyme-linked immunosorbent assay (ELISA) to detect IL-10 (IL-10 ELISA kit; Sanquin, Amsterdam, The Netherlands), IL-12p70 and IL-15 (QuantiGlo ELISA kit, R&D systems).

Cytokine production by MUTZ-3 IDC and LC-stimulated CD8+ and CD4+ T cells

$1x10^6$ CD8β+ T cells and CD8β- PBMC were cultured with either medium alone (un-stimulated) or medium containing $1x10^5$ mature MUTZ-3 IDC or MUTZ-3 LC in the presence of 5 ng/ml IL-7 in a 24 well plate. On day 7, the T cells were re-stimulated with 25 ng/ml PMA and 1 μg/ml ionomycin (Sigma) in the presence of GolgiPlug (BD Biosciences) to detect intracellular production of IFN-γ and IL-4. After 4 hours, cells were harvested, washed, stained with APC-labeled anti-CD8 or anti-CD4 and PerCP-CY.5.5-labeled anti-CD3 mAbs. After fixation and permeabilization, cells were labeled with FITC-labeled anti-IFN-γ mAb (BD Biosciences) and PE-labeled anti-IL-4 mAb. Stained cells were analyzed on a FACScalibur.

Statistical Analysis

Differences between means of percentage of migrated dendritic cells, between means of T cell stimulatory capacity and between means of cytokine production of the different DC subsets were compared using a paired two-sided T-test. Differences between medians of percentage tetramer-positive CD8+ T cells were compared using a two-sided Mann-Whitney test. Differences were considered significant when $p < 0.05$.

Results

Phenotype and allogeneic T Cell Stimulatory Capacity of MUTZ-3-derived IDC and LC.

As shown in figure 1 and described previously (21), MUTZ-3 progenitors are able to differentiate into either IDC, expressing CD1a and DC-SIGN, but lacking Langerin, or LC, expressing CD1a and Langerin, but lacking DC-SIGN (Fig. 1*A*). Upon maturation, up-regulation of co-stimulatory molecules, *de novo* expression of CD83 and enhanced allogeneic T cell stimulation was observed for both MUTZ-3 IDC and LC (21). Of note, expression levels of co-stimulatory and adhesion molecules were generally higher on MUTZ-3 LC (Fig. 1*A*), which translated into a significantly higher proliferation of total PBL in an allo-MLR (Fig. 1*B;* $p < 0,03$). Importantly, this increased proliferation was also observed for isolated CD8β+ CTL precursors (Fig. 1*C;* $p < 0,023$), revealing a superior allogeneic (CD8+) T cell stimulatory capacity for MUTZ-3 LC as compared to MUTZ-3 IDC.

Lymph Node Migration Capacity of MoDC, MUTZ-3 IDC and LC.

DC are professional antigen-presenting cells with the capacity to take up antigen in the periphery and present this antigen in the secondary lymphoid organs. As described, the migration of MoDC is dependent on PGE2 (30-32). To determine whether mature MUTZ-3 IDC and LC are capable of migrating and whether this migration is also dependent on PGE2, MUTZ-3 IDC and LC were analyzed for the expression of the chemokine receptor CCR7 by flow cytometry and for their migratory capacity towards the lymph node-homing chemokines CCL19 and CCL21 in transwell migration assays.

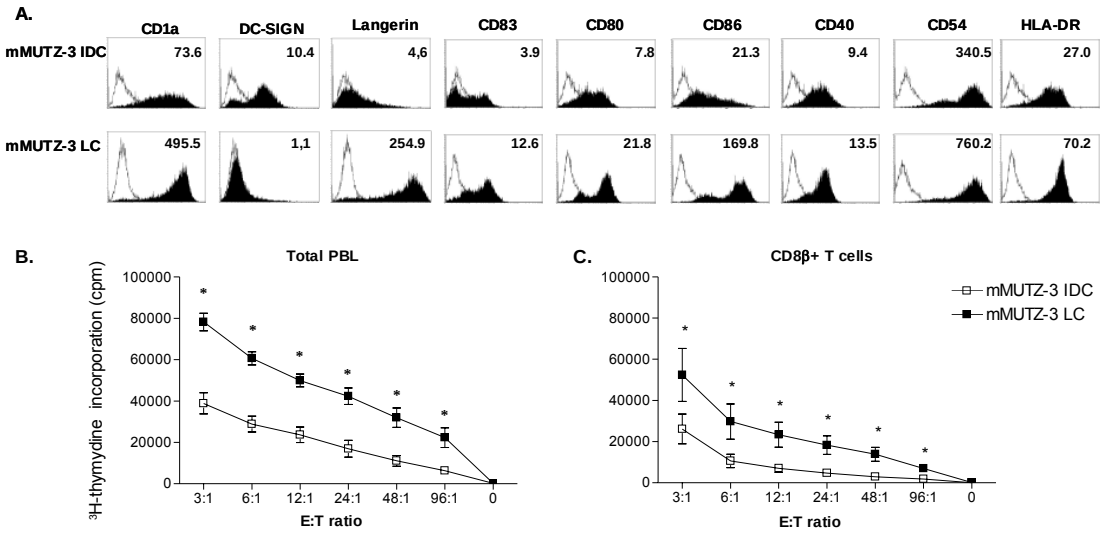

Figure 1. Phenotype and T Cell Stimulatory Capacity of MUTZ-3-derived IDC and LC. Mature CD1a+/DC-SIGN+ MUTZ-3 IDC and CD1a+/Langerin+ MUTZ-3 LC were analyzed for their expression of co-stimulatory and adhesion molecules and their allogeneic T cell stimulatory capacity. Expression levels of CD1a, DC-SIGN, Langerin and several co-stimulatory and adhesion molecules were analyzed by flow cytometry (A). *Open histograms*, isotype-matched controls; *closed histograms*, the marker as indicated above. Mean fluorescence indices are listed in the upper right corner. Allogeneic T cell stimulatory capacity was analyzed by Mixed Lymphocyte Reaction (MLR). Proliferation of total PBL (B) and isolated CD8β+ CTL precursors (C) was assessed by ^{3}H-thymidine incorporation (cpm) after culturing for 5 days with either mature MUTZ-3 IDC or LC. Data shown for MUTZ-3 IDC and LC phenotype is representative of 5 independent experiments, and for the mean proliferation ± SEM of 4 independent experiments. Differences between means of T cell stimulatory capacity of the MUTZ-3 IDC and LC were compared using a paired two-sided T-test and were considered significant when $p < 0.05$, as indicated with an asterisk (*).

To this end, MUTZ-3 IDC, LC and MoDC matured with a cocktail of cytokines (MCM mimic) with or without PGE2, were tested as such. Flow cytometric analysis revealed upregulation of CCR7 on matured MoDC, MUTZ-3 IDC and LC (data not shown), which was accompanied by migration towards lymph node-homing chemokines CCL19 and CCL21 (Fig. 2). No significant differences in the percentage of migrating cells of all three MCM mimic + PGE2-matured DC subtypes were observed. However, in contrast to MoDC and LC, the migration of MUTZ-3 IDC was not dependent on the presence of PGE2 in the maturation cocktail (Fig. 2). Although PGE2 has been described to be a critical component for DC migration, it has been demonstrated recently that immuno-stimulatory DC with lymph node migration and IL-12p70 release capabilities can be generated in the absence of PGE2, by making use of an IFN-α/p-I:C-type-1 cytokine cocktail (26). To this end, IFN-α/p-I:C-type-1-matured MUTZ-3 IDC, LC and MoDC were also tested for their responsiveness towards CCL19 and CCL21. As shown in figure 2, MUTZ-3 IDC were more responsive to CCL19 and CCL21 upon IFN-α/p-I:C-type-1-induced maturation as compared to MoDC and MUTZ-3 LC, underlining the observation that MUTZ-3 IDC are more capable of PGE2-independent migration.

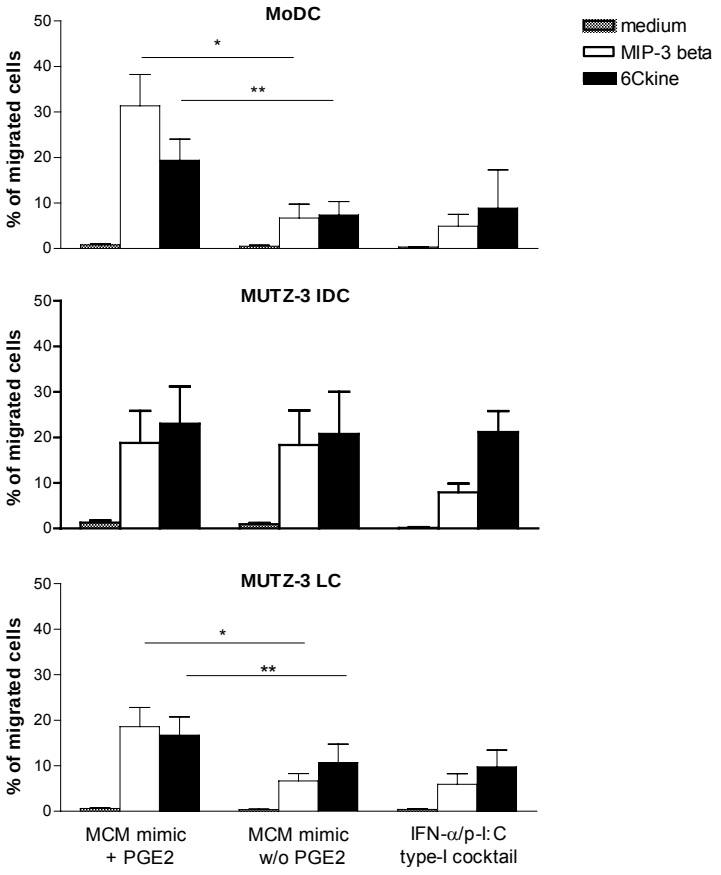

Figure 2. Analysis of migratory capacity of MUTZ-3 IDC, LC and MoDC. MoDC, MUTZ-3 IDC and LC, either immature or matured with MCM mimic with or without PGE2 or with the IFN-α/p-I:C type-1 cytokine cocktail were analyzed for their capacity to migrate towards lymph node homing chemokines CCL19 and CCL21 in a transwell migration assay. Migration towards medium, CCL19 and CCL21 is given as the percentage migrated cells. Data represent the means ± SEM of experiments of 8 separate donors for MoDC *(top panel)* and 6 independent experiments for MUTZ-3 IDC *(middle panel)* and LC *(bottom panel)*. Differences between means of percentage of migrated dendritic cells of the different DC subsets were compared using a paired two-sided T-test and were considered significant when $p < 0.05$, as indicated with an asterisk (*).

Cytokine Secretion by MUTZ-3 IDC, LC and MoDC.

Another important function of fully mature, immuno-stimulatory DC is the ability to produce cytokines important for T helper and cytotoxic T cell activation, like IL-12, IL-23 and IL-15 (33,34), whereas cytokines that play a role in the induction of T cell tolerance, such as IL-10, should preferably

not be produced (35). For that reason, CD40L-stimulated MUTZ-3 IDC, MUTZ-3 LC and MoDC were analyzed for the release of IL-12p70, IL-15, IL-23, and IL-10. Whereas MoDC released considerable amounts (ranging from 2-5 ng/ml) of IL-10 with the maturation methods employed here, no IL-10 was secreted by either MUTZ-3 IDC or MUTZ-3 LC (data not shown). MoDC also secreted higher amounts of IL-12p70 as compared to MUTZ-3 IDC, whereas MUTZ-3 LC did not secrete any detectable IL-12 (Fig. 3A). The IL-12p70 secretion by MoDC was impaired by the addition of PGE2 in the maturation cocktail, although this was not significant. MUTZ-3 IDC, LC and MoDC were also analyzed for the capacity to produce IL-15 and IL-23. As shown in figure 3B, immature and MCM mimic +/- PGE2-matured MUTZ-3 IDC, LC and MoDC hardly produced IL-15, whereas IFN-α/p-I:C type-1 cocktail-matured MoDC and MUTZ-3 IDC, but not MUTZ-3 LC, did produce significantly higher amounts of IL-15. IL-23 was not released at detectable levels by either IDC or LC (data not shown). In summary, CD40L-stimulated MUTZ-3 IDC do release T cell-stimulatory cytokines, albeit at relatively low levels compared to MoDC, whereas LC do not do so at all.

Cytokine profile of MUTZ-3 IDC and LC-stimulated CD8+ and CD4+ T cells.

To study whether the low level or absence of IL-12p70 released by MUTZ-3 IDC and LC respectively, led to a change in cytokine production by T cells, thereby shifting T cells towards a more Th2 cytokine profile, we analyzed MUTZ-3 IDC and LC-stimulated CD8β+ T cells and CD8β-depleted PBL for the production of IL-4 and IFN-γ. As shown in figure 3C, both MUTZ-3 IDC and LC-stimulated CD8+ and CD4+ T cells mainly produced IFN-γ, but not IL-4. Moreover, the production of IFN-γ by CD8+ and CD4+ T cells was significantly increased as compared to un-stimulated CD8+ and CD4+ T cells. Importantly, in all conditions, no IFN-γ/IL-4 double-positive T cells could be detected (data not shown), suggesting that MUTZ-3 IDC and -LC primarily expanded type-1 cytokine-producing T cells, despite the low level or complete absence of IL-12p70 during stimulation.

Induction of Tumor-Specific CD8+ T cells *in vitro* using Peptide-Pulsed HLA-A2-matched MUTZ-3 IDC or MUTZ-3 LC.

DC exhibit the unique capacity to induce and activate tumor-specific CTL both *in vivo* and *in vitro*. We previously described that MUTZ-3 IDC can be used for *in vitro* priming and expansion of functional TAA-specific effector CTL and that the efficiency of this induction was comparable to autologous peptide-loaded MoDC (22). In order to determine whether MUTZ-3 LC were also capable of inducing functional tumor-specific CTL and to see whether the CTL induction efficiency is comparable to that of MUTZ-3 IDC, both IDC and LC were used as stimulator cells in an *in vitro* CTL induction protocol. To this end, HLA-A2+ CD8β+ CTL precursors were stimulated with HLA-A2-matched and peptide-loaded mature MUTZ-3 IDC and MUTZ-3 LC in multiple parallel cultures starting with $1x10^6$ CD8β+ CTL precursors in each culture. Epitopes selected were the immunodominant HLA-A2-restricted MART-1-derived peptide MART-1_{26L}, the CEA-derived peptide CEA_{571}, the Her-2/neu-derived peptide Her-2/neu_{369} and the PSA-derived epitope PSA_{146}. From the second round of stimulation onwards, the presence of tumor-specific CD8+ T cells was monitored by tetramer staining. When stimulated with MUTZ-3 IDC significantly higher levels of MART-1_{26L}-tetramer-positive T cells could be detected after

two IVS compared to MUTZ-3 LC in two of three donors analyzed (Fig. 4*A*). In addition, a similar trend was also observed for the adenocarcinoma-associated peptides CEA_{571}, PSA_{146} and Her-2/neu_{369}, in number of tetramer-positive cultures (17/48 versus 9/48 individual cultures for MUTZ-3 IDC and LC respectively), as well as in higher detectable maximum tetramer-positive T cell frequencies (Fig. 4*B*), although these differences did not reach statistical significance.

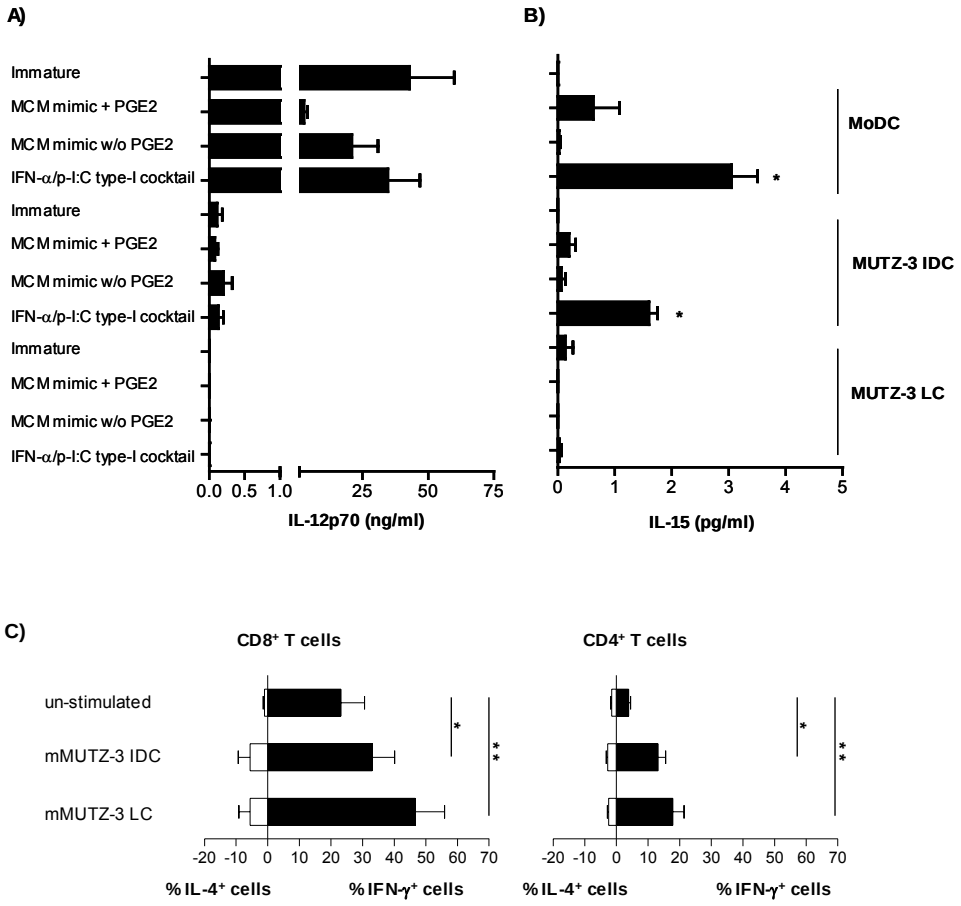

Figure 3. Cytokine secretion by MUTZ-3 IDC, LC and MoDC (IL-12p70 and IL-15) and MUTZ-3 IDC and LC-stimulated CD8+ and CD4+ T cells (IFNγ and IL-4). MoDC, MUTZ-3 IDC and LC were analyzed for the production of IL-12p70 and IL-15. For IL-12 production, DC were left untreated or stimulated for 8 hours with either MCM mimic + PGE2, MCM mimic w/o PGE2 or the IFN-α/p-I:C type-1 cytokine cocktail, followed by an 18 hour stimulation with CD40L-transfected J558 cells in the presence of 1000 U/ml IFN-γ. For IL-15 production, DC were left untreated or stimulated for 18 hours with either MCM mimic + PGE2, MCM mimic w/o PGE2 or the IFN-α/p-I:C type-1 cytokine cocktail. IL-12p70 production **(A)** and IL-15 production **(B)** by MoDC (*left panel*) MUTZ-3 IDC (*middle panel*) and MUTZ-3 LC (*right panel*). Amount of IL-12p70 is given at a cell concentration of $1x10^5$ DC/ml and amount of IL-15 at a cell concentration of $1x10^6$ DC/ml. Data represent the means ± SEM of 4 different donors. **(C)** MUTZ-3 IDC and LC-stimulated CD8+ and CD4+ T cells were analyzed for their capacity to produce IFN-γ and IL-4 by intracellular cytokine staining. CD8β+ T cells and $CD8\beta^-$ PBMC were cultured for 7 days with either medium (un-stimulated) or MCM mimic + PGE2-matured MUTZ-3 IDC or LC, followed by a four hour stimulation with PMA and ionomycin and analyzed for the production of IL-4 and IFN-γ. Percentage of IFN-γ+ and IL-4+ cells were gated for live CD3+/CD8+ or live CD3+/CD4+ T cells. Data represent the means ± SEM of 4 independent experiments of CD8+ T cells (*left panel*) and CD4+ T cells (*right panel*). Differences between means of IL-12p70 and IL-15 production of the different DC subsets and between means of percentage of IFNγ and or IL-4 production of MUTZ-3 IDC and LC-stimulated T cells were compared using a paired two-sided T-test and were considered significant when $p < 0.05$, as indicated with an asterisk (*).

Although functionally active, functional avidity of the MUTZ-3 IDC and LC-generated MART-1_{26L}- and Her-2/neu_{369}-specific CD8+ T cells were relatively low. Both MUTZ-3 IDC and LC-generated MART-1_{26L}- and Her-2/neu_{369}-specific CD8+ T cells were able to recognize exogenously loaded MART-1_{26L}- and Her-2/neu_{369} target cells respectively, but recognition of endogenously processed and presented MART-1_{26L} and Her-2/neu_{369} on tumor cells was low, as analyzed by intracellular IFN-γ (Fig. 4*C*) and ^{51}chromium release assays (Fig. 4*D*).

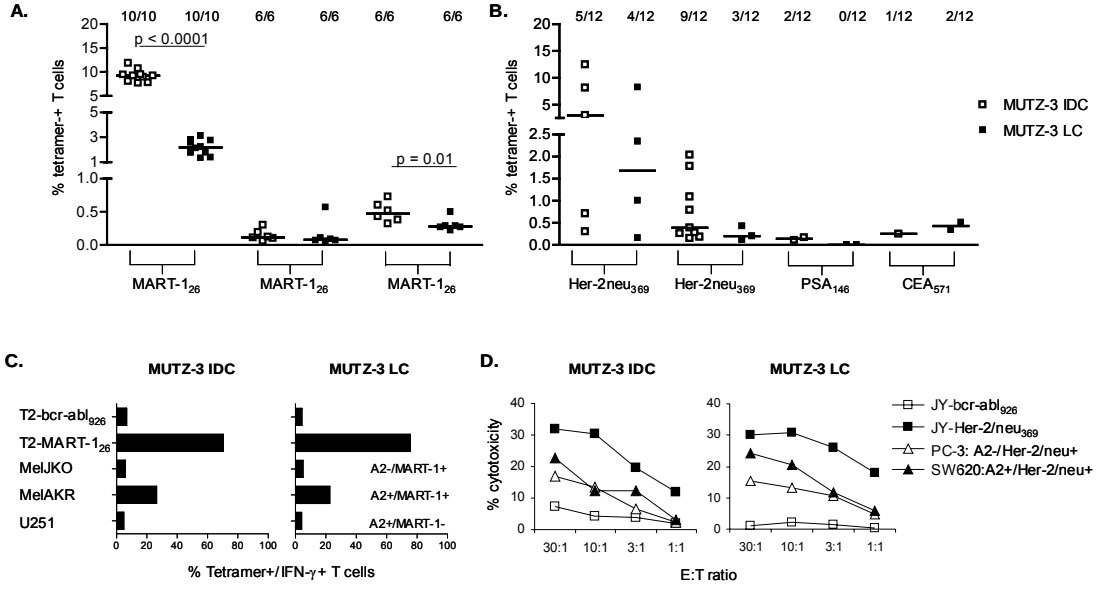

Figure 4. Flow cytometric HLA-A2+ tetramer (Tm)-binding and functional analysis of MUTZ-3 IDC and LC-derived tumor antigen-specific CD8+ T cells. The induction of tumor antigen-specific (i.e. MART-1_{26L}, Her-2/neu_{369}, CEA_{571} and PSA_{146}-specific) CD8+ T cells was monitored by tetramer analysis. Percentage of MART-1_{26L}-tetramer-positive CD8+ T cells achieved after two *in vitro* stimulation (IVS) (A) or maximum percentage of Her-2/neu_{369}, CEA_{571} and PSA_{146}-tetramer-positive CD8+ T cells after multiple IVS (B) with either MUTZ-3 IDC *(closed circles)* or LC *(open circles)* is depicted. Differences between medians of percentage tetramer-positive CD8+ T cells from MUTZ-3 IDC or LC-stimulated cultures were compared using a two-sided Mann Whitney test and were considered significant when $p < 0.05$. Number of tetramer-positive cultures per total number of cultures started is given for each DC subset. Functional activity of MUTZ-3 IDC and LC-generated CD8+ T cells was determined by intracellular IFNγ assay (C) or standard ^{51}chromium release assay (D). Target cells used were HLA-A2+ JY cells loaded with either MART-1_{26L} peptide or with control HLA-A2-restricted peptide Bcr-abl_{926}, the HLA-A2-/MART-1+ cell line Mel-JKO, the HLA-A2+/MART-1+ cell line Mel-AKR and the HLA-A2+/MART-1- cell line U251 (C) or HLA-A2+ JY cells loaded with either Her-2/neu_{369} peptide or with control HLA-A2-restricted peptide Bcr-abl_{926}, the HLA-A2+/Her-2/neu+ cell line SW620 and the HLA-A2-/Her-2/neu+ cell line PC-3 (D).

As described, type-1 T cell stimulatory cytokines such as IL-12 are important in functional T cell priming. In order to determine whether the reduced CD8+ T cell priming efficiency of MUTZ-3 LC might be related to the inability of LC to produce type 1 stimulatory cytokines, IL-12p70 was introduced into MUTZ-3 cells by retroviral transduction, and IDC and LC derived from these MUTZ-3-IL-12 cells were analyzed for their CD8+ T cells priming capacity. Il-12p70 production by MUTZ-3-IL-12 IDC and LC was confirmed and ranged between 1.0 - 1.7 ng/ml per 200,000 cells per 24 hours (data not shown). As shown in figure 5*A*, CD8+ T cell priming efficiency of MUTZ-3-IL-12 IDC and LC was significantly increased compared to MUTZ-3 IDC and LC, as indicated by the generation of enhanced levels of MART-1_{26L}-specific CD8+ T cells. Moreover, introducing IL-12p70 also enhanced the

functional avidity and tumor cell recognizing abilities of the generated CD8+ T cells. Whereas MART-1_{26L}-specific CD8+ T cells primed with MUTZ-3 IDC and LC exhibited only intermediate functional avidity (fig. 5*B*; *open symbols*), MUTZ-3-IL-12 IDC and LC-generated MART-1_{26L}-specific CD8+ T cells exhibited high functional avidity (fig. 5*B*, *closed symbols*). The increased functional avidity of the MUTZ-3-IL-12 IDC and IL-12 LC-generated CD8+ T cells resulted in an increased capacity to recognize endogenously expressed MART-1_{26} on tumor cells as measured by intracellular IFN-γ (Fig. 5*C*) and ^{51}chromium release assay (Fig. 5*D*). Indeed, MUTZ-3-IL-12 IDC (data not shown) and IL-12 LC-generated MART-1_{26L}-specific CD8+ T cells (Fig 5D; right panel) were both able to specifically recognize and kill the HLA-A2+/MART-1+ tumor cell line Mel-AKR, whereas MUTZ-3 IDC (not shown) and LC-generated MART-1_{26L}-specific CD8+ T cells (Fig. 5D; left panel) were not. In addition, MART-1_{26L} -specific CD8+ T cells induced with MUTZ-3-IL-12 IDC/LC also showed a reduced expression of CD27, CD28, CD62L and CCR7 compared to MUTZ-3 IDC/LC stimulated MART-1_{26L}-specific CD8+ T cells, indicative of a more advanced effector T cell differentiation (data not shown).

In summary, *in vitro* functions of IDC and LC suggest that both DC subsets can serve as valid vaccine vehicles for tumor immunotherapy, particularly after provision of type-1 T cell stimulatory cytokines.

Discussion

Because of their critical role in orchestrating the immune response, dendritic cells are increasingly applied as vaccines for the treatment of cancer (17). So far, in the majority of clinical trials, MoDC have been used for vaccination. However, it has been described recently that CD34-derived LC exhibit superior T cell priming capacity over CD34-derived IDC and MoDC *in vitro*, suggesting a potential benefit of the use of LC in clinical DC vaccination. In this study, extensive characterization of the functional differences between IDC and LC was performed by making use of the MUTZ-3 cell line as a model system. We show here that both DC subsets are capable of inducing anti-tumor T cell immunity and provide valid vaccine vehicles for tumor immunotherapy, albeit that provision of IL-12p70 is required to ensure optimal T cell stimulation. As described previously, employing allogeneic MUTZ-3 IDC as stimulator cells in an *in vitro* induction protocol, functional tumor-specific CTL could be generated (22).

In this study, by employing the same method, we confirmed previous findings of the applicability of allogeneic HLA-A2-matched MUTZ-3 IDC. Although mature LC showed significantly higher allogeneic T cell stimulatory capacity, IDC supported the induction of tumor antigen-specific CD8+ T cells at an overall higher efficiency as compared to LC. This was not in line with findings from other groups, demonstrating superior CTL priming capacity of CD34-derived LC over CD34-derived IDC or MoDC (15,19). Discrepancies might be explained by the fact that we made use of an allogeneic T cell activation system. Indeed, the observed enhanced allogeneic T cell stimulatory capacity of MUTZ-3 LC, as compared to MUTZ-3 IDC, may account for the decreased CTL priming capacity, with possible preferential outgrowth of non-specific T cells. Of note, comparing the induction efficiency of autologous

MoDC and allogeneic MUTZ-3 IDC (22), we previously did not find evidence for this allogeneic response interfering with the antigen-specific CTL response.

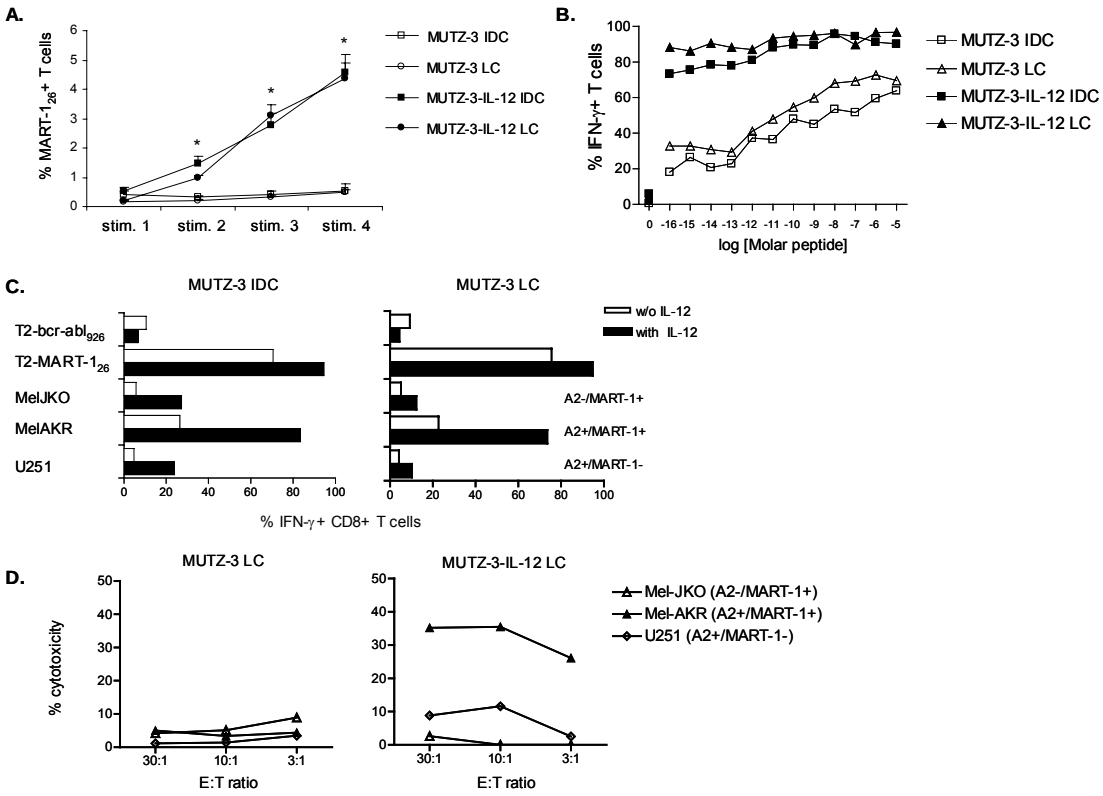

Figure 5. Flow cytometric HLA-A2+ tetramer (Tm)-binding and functional analysis of MUTZ-3-IL-12 IDC and LC-derived MART-1-specific CD8+ T cells. The induction of MART-1_{26}-specific CD8+ T cells was monitored by tetramer analysis. Percentage of tetramer-positive CD8+ T cells achieved after four *in vitro* stimulation rounds (A) with either MUTZ-3 IDC, LC, IL12 IDC or IL-12 LC is depicted. Data represent the medians ± SEM of experiments of 3 separate donors for MUTZ-3 LC, MUTZ-3-IL-12 IDC and -IL-12 LC and 2 independent experiments for MUTZ-3 IDC. Differences between medians of percentage of tetramer-positive CD8+ T cells from MUTZ-3 IDC, MUTZ-3-IL12 IDC, MUTZ-3 LC or MUTZ-3-IL-12 LC-stimulated cultures were compared using a two-sided Mann Whitney test and were considered significant when $p < 0.05$, as indicated with an asterisk (*). Functional avidity (B) and lytic activity (C and D) of MUTZ-3 IDC, LC, -IL-12 IDC and -IL-12 LC- generated CD8+ T cells was determined by intracellular IFNγ assay or standard ^{51}chromium release assay. Target cells used were HLA-A2+ JY cells loaded with either serial 10-fold dilutions of MART-1_{26L} peptide or with a fixed dose of MART-1_{26L} or control peptide Bcr-abl$_{926}$, the HLA-A2-/MART-1+ cell line Mel-JKO, the HLA-A2+/MART-1+ cell line Mel-AKR and the HLA-A2+/MART-1- glioma cell line U251.

The superior tumor-antigen-specific CD8+ T cell induction of IDC might also be related to the observed inability of LC to release T cell stimulatory cytokines such as IL-12p70, IL-15 and IL-23. Although no differences were observed in the cytokine expression profile of IDC and LC primed T cells, transduction with IL-12p70 significantly improved the priming efficiency of both IDC and LC and abrogated the difference in tumor-specific CD8+ priming efficiency between the DC subsets. Moreover, introducing IL-12p70 also resulted in a more advanced effector T cell differentiation with enhanced functional avidity and tumor cell recognizing abilities of the IDC and LC generated CD8+ T cells, as also recently described by us using mRNA-transfected MoDC (36).

The low level or absence of pro-inflammatory cytokine production by MUTZ-3 IDC and LC as compared to MoDC might be explained by the leukemic origin of the MUTZ-3 cell line, since AML-blast-derived DC are described to produce only low amounts of IL-12 (37). However, the observation that MUTZ-3 IDC and LC do not produce any IL-10 with the maturation cocktails employed in this study, argues against a possible immunosuppressive phenotype. Moreover, the low level or absence of IL-12p70 production is consistent with recently described findings that skin-migrated IDC and LC, as well as CD34-derived IDC and LC, also do not produce IL-12p70 (19,38,39).

A pivotal role of fully mature, immuno-stimulatory DC is the ability of DC to migrate to the draining lymph nodes. Upon maturation, CCR7 expression was induced on MUTZ-3 IDC and LC and this expression was accompanied by responsiveness to lymph node-homing chemokines CCL19 and CCL21. Interestingly, and unlike migration of MoDC (30,31), migration of MUTZ-3 IDC and LC was independent (IDC) or less dependent (LC) on PGE2. Importantly, so far it is not clear whether CD34-derived IDC or LC migration is dependent on PGE2. Of note, PGE2 dependence for MoDC migration could be confirmed in our experiments, thereby validating our migration assay. Furthermore, the particular high migration of MUTZ-3 IDC in response to CCL19 and CCL21 upon maturation with the IFN-α/p-I:C-type-1 cocktail also underlines this PGE2-independence (26). Since PGE2 has been described as an inflammatory mediator with a Th2 driving role (40,41), the ability of MUTZ-3 IDC and LC to migrate independent of PGE2 towards lymph node homing chemokines might be beneficial in clinical DC vaccination settings.

Taken together, comparative functional analysis of MUTZ-3 derived IDC and LC revealed that, except for the inability of LC to release distinct type-1 T cell stimulatory cytokines, both DC subsets exhibit functional properties that are essential for the *in vivo* generation of CTL mediated immunity. In conclusion, both DC subsets are valid vaccine vehicles for tumor immunotherapy, but provision of type-1 T cell stimulatory cytokines such as IL-12p70 may be required to ensure optimal T cell stimulation.

References

1. Banchereau J, Briere F, Caux C, et al. Immunobiology of dendritic cells. Annu Rev Immunol 2000;18:767-811.
2. Steinman RM. The dendritic cell system and its role in immunogenicity. Annu Rev Immunol 1991;9:271-96.
3. Lanzavecchia A, Sallusto F. Regulation of T cell immunity by dendritic cells. Cell 2001;106:263-6.
4. Caux C, Vanbervliet B, Massacrier C, et al. CD34+ hematopoietic progenitors from human cord blood differentiate along two independent dendritic cell pathways in response to GM-CSF+TNF alpha. J Exp Med 1996;184:695-706.
5. Caux C, Massacrier C, Vanbervliet B, et al. CD34+ hematopoietic progenitors from human cord blood differentiate along two independent dendritic cell pathways in response to granulocyte-macrophage colony-stimulating factor plus tumor necrosis factor alpha: II. Functional analysis. Blood 1997;90:1458-70.
6. Flamand V, Sornasse T, Thielemans K, et al. Murine dendritic cells pulsed in vitro with tumor antigen induce tumor resistance in vivo. Eur J Immunol 1994;24:605-10.
7. Ossevoort MA, Feltkamp MC, van Veen KJ, Melief CJ, Kast WM. Dendritic cells as carriers for a cytotoxic T-lymphocyte epitope-based peptide vaccine in protection against a human papillomavirus type 16-induced tumor. J Immunother Emphasis Tumor Immunol 1995;18:86-94.
8. Celluzzi CM, Mayordomo JI, Storkus WJ, Lotze MT, Falo LD, Jr. Peptide-pulsed dendritic cells induce antigen-specific CTL-mediated protective tumor immunity. J Exp Med 1996;183:283-7.
9. Mayordomo JI, Zorina T, Storkus WJ, et al. Bone marrow-derived dendritic cells pulsed with synthetic tumour peptides elicit protective and therapeutic antitumour immunity. Nat Med 1995;1:1297-302.
10. Hsu FJ, Benike C, Fagnoni F, et al. Vaccination of patients with B-cell lymphoma using autologous antigen-pulsed dendritic cells. Nat Med 1996;2:52-8.
11. Fong L, Hou Y, Rivas A, et al. Altered peptide ligand vaccination with Flt3 ligand expanded dendritic cells for tumor immunotherapy. Proc Natl Acad Sci U S A 2001;98:8809-14.
12. Shortman K, Liu YJ. Mouse and human dendritic cell subtypes. Nat Rev Immunol 2002;2:151-61.
13. Nestle FO, Alijagic S, Gilliet M, et al. Vaccination of melanoma patients with peptide- or tumor lysate-pulsed dendritic cells. Nat Med 1998;4:328-32.
14. Thurner B, Haendle I, Roder C, et al. Vaccination with mage-3A1 peptide-pulsed mature, monocyte-derived dendritic cells expands specific cytotoxic T cells and induces regression of some metastases in advanced stage IV melanoma. J Exp Med 1999;190:1669-78.
15. Banchereau J, Palucka AK, Dhodapkar M, et al. Immune and clinical responses in patients with metastatic melanoma to CD34(+) progenitor-derived dendritic cell vaccine. Cancer Res 2001;61:6451-8.
16. Mackensen A, Herbst B, Chen JL, et al. Phase I study in melanoma patients of a vaccine with peptide-pulsed dendritic cells generated in vitro from CD34(+) hematopoietic progenitor cells. Int J Cancer 2000;86:385-92.
17. Davis ID, Jefford M, Parente P, Cebon J. Rational approaches to human cancer immunotherapy. J Leukoc Biol 2003;73:3-29.
18. Ferlazzo G, Wesa A, Wei WZ, Galy A. Dendritic cells generated either from CD34+ progenitor cells or from monocytes differ in their ability to activate antigen-specific CD8+ T cells. J Immunol 1999;163:3597-604.
19. Ratzinger G, Baggers J, de Cos MA, et al. Mature human Langerhans cells derived from CD34+ hematopoietic progenitors stimulate greater cytolytic T lymphocyte activity in the absence of bioactive IL-12p70, by either single peptide presentation or cross-priming, than do dermal-interstitial or monocyte-derived dendritic cells. J Immunol 2004;173:2780-91.
20. Masterson AJ, Sombroek CC, De Gruijl TD, et al. MUTZ-3, a human cell line model for the cytokine-induced differentiation of dendritic cells from CD34+ precursors. Blood 2002;100:701-3.
21. Santegoets SJ, Masterson AJ, van der Sluis PC, et al. A CD34+ human cell line model of myeloid dendritic cell differentiation: evidence for a CD14+CD11b+ Langerhans cell precursor. J Leukoc Biol 2006;80:1337-44.
22. Santegoets SJ, Schreurs MW, Masterson AJ, et al. In vitro priming of tumor-specific cytotoxic T lymphocytes using allogeneic dendritic cells derived from the human MUTZ-3 cell line. Cancer Immunol Immunother 2006;55:1480-90.
23. Schreurs MW, Scholten KB, Kueter EW, Ruizendaal JJ, Meijer CJ, Hooijberg E. In vitro generation and life span extension of human papillomavirus type 16-specific, healthy donor-derived CTL clones. J Immunol 2003;171:2912-21.

24. Bontkes HJ, Ruizendaal JJ, Kramer D, et al. Constitutively active STAT5b induces cytokine-independent growth of the acute myeloid leukemia-derived MUTZ-3 cell line and accelerates its differentiation into mature dendritic cells. J Immunother 2006;29:188-200.
25. Bender A, Sapp M, Schuler G, Steinman RM, Bhardwaj N. Improved methods for the generation of dendritic cells from nonproliferating progenitors in human blood. J Immunol Methods 1996;196:121-35.
26. Mailliard RB, Wankowicz-Kalinska A, Cai Q, et al. alpha-type-1 polarized dendritic cells: a novel immunization tool with optimized CTL-inducing activity. Cancer Res 2004;64:5934-7.
27. Heemskerk MH, Hooijberg E, Ruizendaal JJ, et al. Enrichment of an antigen-specific T cell response by retrovirally transduced human dendritic cells. Cell Immunol 1999;195:10-7.
28. Yssel H, de Vries JE, Koken M, Van Blitterswijk W, Spits H. Serum-free medium for generation and propagation of functional human cytotoxic and helper T cell clones. J Immunol Methods 1984;72:219-27.
29. Vieira PL, De Jong EC, Wierenga EA, Kapsenberg ML, Kalinski P. Development of Th1-inducing capacity in myeloid dendritic cells requires environmental instruction. J Immunol 2000;164:4507-12.
30. Luft T, Jefford M, Luetjens P, et al. Functionally distinct dendritic cell (DC) populations induced by physiologic stimuli: prostaglandin E(2) regulates the migratory capacity of specific DC subsets. Blood 2002;100:1362-72.
31. Scandella E, Men Y, Legler DF, et al. CCL19/CCL21-triggered signal transduction and migration of dendritic cells requires prostaglandin E2. Blood 2004;103:1595-601.
32. Scandella E, Men Y, Gillessen S, Forster R, Groettrup M. Prostaglandin E2 is a key factor for CCR7 surface expression and migration of monocyte-derived dendritic cells. Blood 2002;100:1354-61.
33. Becker TC, Wherry EJ, Boone D, et al. Interleukin 15 is required for proliferative renewal of virus-specific memory CD8 T cells. J Exp Med 2002;195:1541-8.
34. Cella M, Scheidegger D, Palmer-Lehmann K, Lane P, Lanzavecchia A, Alber G. Ligation of CD40 on dendritic cells triggers production of high levels of interleukin-12 and enhances T cell stimulatory capacity: T-T help via APC activation. J Exp Med 1996;184:747-52.
35. Groux H, Bigler M, de Vries JE, Roncarolo MG. Interleukin-10 induces a long-term antigen-specific anergic state in human CD4+ T cells. J Exp Med 1996;184:19-29.
36. Bontkes HJ, Kramer D, Ruizendaal JJ, et al. Dendritic cells transfected with interleukin-12 and tumor-associated antigen messenger RNA induce high avidity cytotoxic T cells. Gene Ther 2007;14:366-75.
37. Curti A, Pandolfi S, Aluigi M, et al. Interleukin-12 production by leukemia-derived dendritic cells counteracts the inhibitory effect of leukemic microenvironment on T cells. Exp Hematol 2005;33:1521-30.
38. Ebner S, Ratzinger G, Krosbacher B, et al. Production of IL-12 by human monocyte-derived dendritic cells is optimal when the stimulus is given at the onset of maturation, and is further enhanced by IL-4. J Immunol 2001;166:633-41.
39. Munz C, Dao T, Ferlazzo G, de Cos MA, Goodman K, Young JW. Mature myeloid dendritic cell subsets have distinct roles for activation and viability of circulating human natural killer cells. Blood 2005;105:266-73.
40. Demeure CE, Yang LP, Desjardins C, Raynauld P, Delespesse G. Prostaglandin E2 primes naive T cells for the production of anti-inflammatory cytokines. Eur J Immunol 1997;27:3526-31.
41. Kalinski P, Hilkens CM, Snijders A, Snijdewint FG, Kapsenberg ML. IL-12-deficient dendritic cells, generated in the presence of prostaglandin E2, promote type 2 cytokine production in maturing human naive T helper cells. J Immunol 1997;159:28-35.
42. de Gruijl TD, Sombroek CC, Lougheed SM, et al. A postmigrational switch among skin-derived dendritic cells to a macrophage-like phenotype is predetermined by the intracutaneous cytokine balance. J Immunol 2006;176:7232-42.

Addendum: data added in proof

In response to reviewers' comments about verifying the abovementioned findings in a more physiological setting, we decided to analyze allogeneic and tumor antigen-specific T cell stimulatory properties and the LN migratory potential of human skin-derived DDC and LC.

Materials and Methods:

Isolation of Dermal Dendritic Cells and Langerhans Cells from Skin

Human HLA-$A2^+$ skin specimens were obtained from healthy donors undergoing corrective breast or abdominal plastic surgery after informed consent. 3-mm thick slices of skin containing both the epidermis and the dermis were cut by use of a dermatome. Slices of skin were cut in pieces of 1 cm2 and incubated with 2.4 U/ml Dispase II (Roche Diagnostics, Mannheim, Germany) for 30 minutes at 37ºC. The epidermis and dermis were separated with tweezers and subsequently (separately) cultured in IMDM complete medium supplemented with 1000 U/ml GM-CSF and 10 ng/ml IL-4 for 48 hours, after which the epidermal and dermal sheets were removed. After 48-72 hours, epidermis- and dermis-migrated cells were harvested, counted, and % CD1a+ cells within these populations was determined by flow cytometry.

Phenotypic and functional analysis of skin-emigrated DDC and LC.

Phenotype of epidermis- and dermis-emigrated DDC and LC was analyzed by flow cytometry. For further functional analysis, the amount of DDC/LC used was calculated based on the expression of the pan-skin DC marker CD1a. Allogeneic T cell stimulatory capacity was determined by MLR as described above. Lymph node-homing capabilities of skin-emigrated DDC and LC was determined by transwell migration assay. To this end, 25,000 skin-emigrated DDC and LC were allowed to migrate towards serum-free medium alone or serum-free medium containing 250 ng/ml of the chemokines CCL19 or CCL21. After 18 hours, the percentage of migrated CD1a+ DDC and LC was determined by fluorescent flow count bead-mediated counting on a flow cytometer. *In vitro* tumor-specific CTL-inducing capabilities of skin-emigrated DDC and LC was determined as described above, with some minor modifications. In brief, multiple bulk cultures of $1x10^6$ CD8β+ T precursors were cultured with $5x10^4$ MART-1_{26L} peptide-loaded CD1a+ skin DDC or LC and with $1x10^6$ irradiated (80 Gy) CD8β- autologous PBMC in Yssel's medium supplemented with 1% hAB serum (ICN Biochemicals), 10 ng/ml IL-6 and 10 ng/ml IL-12 in a 24 well tissue-culture plate. At day 1, 10 ng/ml IL-10 (R&D Systems, Minneapolis, MN) was added. After 10 days, CD8+ T cell cultures were analyzed for the presence of MART-1_{26L}-specific CD8+ T cells by tetramer staining.

Results and Discussion

Analysis of T cell stimulatory properties of human skin-derived DDC and LC

Human skin-emigrated DDC and LC were analyzed for the expression of co-stimulatory and adhesion molecules, their allogeneic and tumor antigen-specific stimulatory capacity and their LN

migratory potential. DDC and LC were obtained from human skin samples by active migration from dermal and epidermal sheets. As described previously by us (42), LC migrating from epidermis represent “true” LC as demonstrated by the expression of Langerin and typical high levels of CD1a, whereas DDC migrated from dermis represent “true” DDC, displaying only intermediate levels of CD1a and no Langerin at the cell membrane and expressing DC-SIGN mRNA. Purity of CD1a+-skin-emigrated DDC and LC in migrated skin cells ranged between 15 and 45 % (data not shown). Furthermore, skin-emigrated DDC and LC displayed a mature phenotype, expressing intermediate-to-high levels of co-stimulatory and adhesion molecules, as well as the maturation marker CD83 (figure 6*A*), and exhibited allogeneic T cell stimulatory capabilities, as demonstrated by allo-MLR (Figure 6*B*). Of note, different from MUTZ-3-derived IDC and LC, no difference in activation status and allogeneic T cell stimulation was observed between the two skin-derived DC subsets.

Skin DDC and LC were also analyzed for their migratory capacity towards lymph node-homing chemokines. As demonstrated in figure 6*C*, mature skin-emigrated DDC were able to migrate towards MIP-3β, whereas migration of mature skin-emigrated LC towards this chemokine was only low. Interestingly, although skin-emigrated DDC and LC were able to migrate towards 6Ckine, percentages were rather low. This may be explained by absence of exogenously added PGE2 both during maturation induction (over 48h of culture of the epidermal and dermal sheets in the presence of GM-CSF and IL-4) and subsequently during migration in the trans-well set-up. Of note, expression of CCR7 was confirmed by flow cytometry as shown in figure 6*A*.

Finally, tumor antigen-specific CTL induction capabilities of both skin DDC and LC were also analyzed. To this end, skin DDC and LC were used as stimulator cells in our *in vitro* CTL induction protocol. As demonstrated in figure 6*D*, both skin-emigrated DDC and LC were capable of inducing MART-1_{26L}-specific CD8+ T cells *in vitro*. Similar as for MUTZ-3-derived IDC and LC (figure 4*A*), significantly higher levels of MART-1_{26L}-specific CD8+ T cells could be detected when stimulated with skin DDC in two of three donors analyzed (figure 6*D*), indicating superior CD8+ T cell priming efficiency of skin DDC compared to skin LC. Our observation that both MUTZ-3 IDC and skin DDC display superior CTL priming capacity over MUTZ-3 LC and skin LC is not in line with findings from other groups, reporting superior CTL priming capacity of CD34-derived LC over CD34-derived IDC or MoDC (15,19). Whereas for MUTZ-3 IDC and LC this discrepancy could be explained by the observed enhanced allogeneic T cell stimulatory capacity of MUTZ-3 LC as compared to MUTZ-3 IDC (figure 1*B* and *C*), possibly resulting in preferential outgrowth of non-specific T cells, our data clearly show that this cannot explain the observed differences in CTL priming efficiency by primary skin-derived DDC and LC (figure 6*B*). Alternatively, differences in CTL priming potential might be related to differences in the production of pro-inflammatory cytokines as also described for CD34-derived IDC and LC (19). Similarly, primary skin-derived LC have been reported to be deficient in IL-12 production (43,44). To ascertain the precise roles of such cytokines in CTL priming by primary LC and DDC, additional investigations are required. Of note, functional avidity analysis revealed no significant difference in functional activity between the skin DDC- and LC-generated MART-1_{26L}-specific CD8+ T cells (figure 6*E*).

In summary, the relative CD8+ T cell induction capacities of skin-derived primary DDC and LC accurately reflect our findings for MUTZ-3 IDC and LC, further validating the MUTZ-3 as a human DDC/LC-equivalent cell line model and demonstrating that both DC subsets can serve as valid vaccine vehicles for tumor immunotherapy.

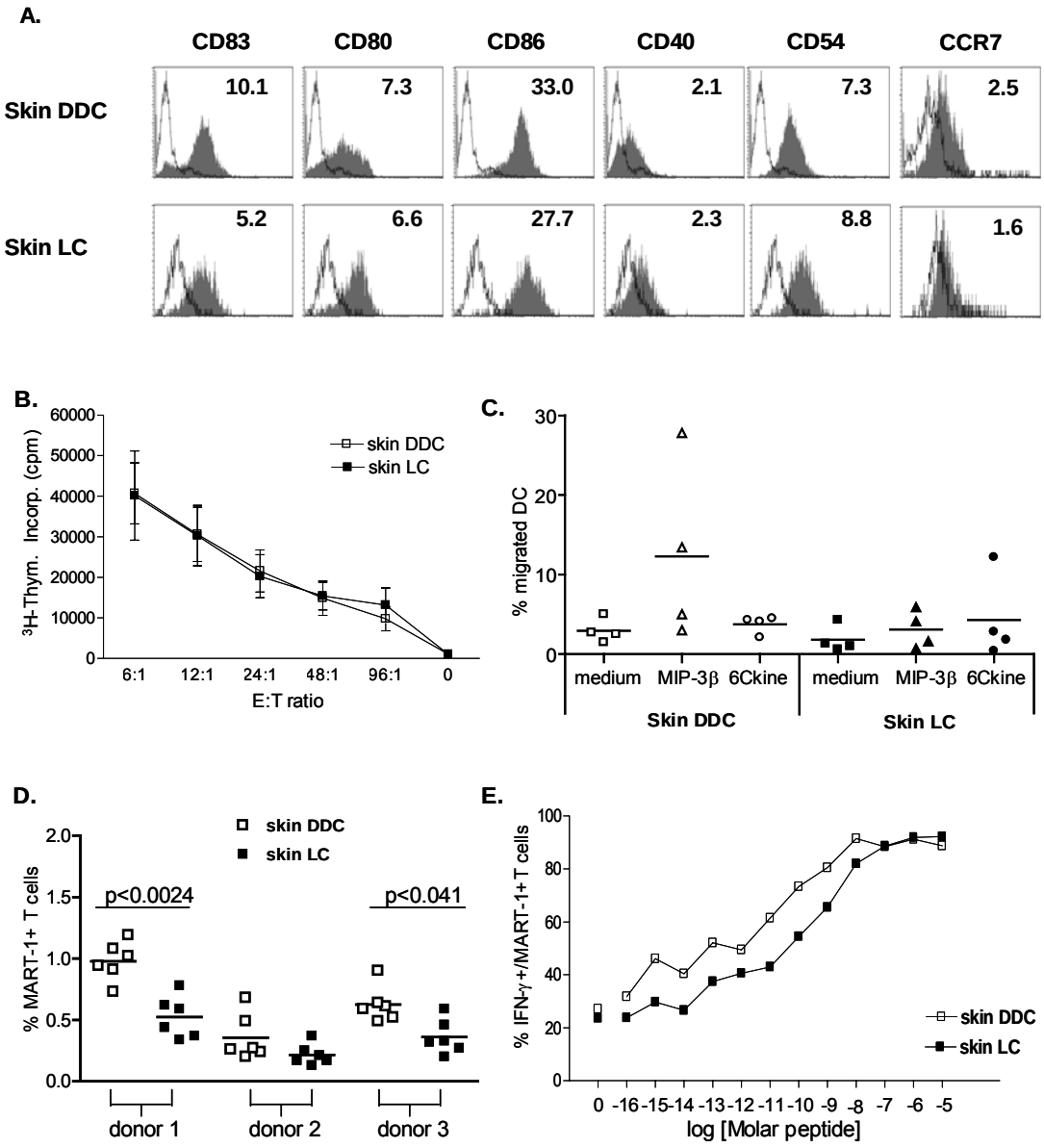

Figure 6. Phenotype and functional analysis of skin-derived DDC and LC. Dermis- and epidermis-emigrated and matured DDC and LC were analyzed for the expression of co-stimulatory and adhesion molecules and their allogeneic T cell stimulatory capacity (A and B), their LN migratory potential (C) and their tumor antigen-specific CD8+ T cell stimulatory potential (D and E). (A) Expression levels of CD83,CD80, CD86, CD40, CD54 and CCR7 were analyzed by flow cytometry. *Open histograms*, isotype-matched controls; *grey histograms*, the marker as indicated above. Mean fluorescence indices are listed in the upper right corner. (B) Allogeneic T cell stimulatory capacity was analyzed by Mixed Lymphocyte Reaction (MLR). Data shown for skin DDC and LC are representative of 4 independent experiments (i.e. donors), and represent means±SEM of quadruplicates. (C) Skin DDC and LC were analyzed for their capacity to migrate towards lymph node homing chemokines MIP-3β and 6Ckine in a transwell migration assay. Migration is given as the percentage migrated cells. Data represent the means±SEM of experiments of 4 separate donors. (D). The induction of MART-1_{26L}-specific CD8+ T cells was monitored by HLA tetramer analysis. Percentage of MART-1_{26L}-tetramer-positive CD8+ T cells achieved after one *in vitro* stimulation with either skin DDC *(open squares)* or LC *(closed squares)* is

depicted. (E). Functional activity of skin DDC and LC-generated CD8+ T cells was determined by intracellular IFNγ assay. Target cells used were HLA-A2+ JY cells loaded with serial 10-fold dilutions of MART-1_{26L} peptide. Differences between means of T cell stimulatory capacity, between means of percentage migrated cells and between means of percentage tetramer-positive CD8+ T cells were compared using a two-sided t-test and were considered significant when $p < 0.05$.

References

43. Peiser, M., R. Wanner, and G. Kolde. 2004. Human epidermal Langerhans cells differ from monocyte-derived Langerhans cells in CD80 expression and in secretion of IL-12 after CD40 cross-linking. J.Leukoc.Biol. 76:616-622.

44. Morelli, A. E., J. P. Rubin, G. Erdos, O. A. Tkacheva, A. R. Mathers, A. F. Zahorchak, A. W. Thomson, L. D. Falo, Jr., and A. T. Larregina. 2005. CD4+ T cell responses elicited by different subsets of human skin migratory dendritic cells. J.Immunol. 175:7905-7915.